Reactivity of Diphenylacetylene with a Basal Edge-Bridged Square-Pyramidal Hexaruthenium Cluster. Characterization of Penta-, Hexa-, and Heptanuclear Alkyne Derivatives

Javier A. Cabeza,*,† Ignacio del Río,† Pablo García-Álvarez,† and Daniel Miguel‡

Departamento de Química Orgánica e Inorgánica, Instituto de Química Organometálica "Enrique Moles", Universidad de Oviedo-CSIC, E-33071 Oviedo, Spain, and Área de Química Inorgánica, Facultad de Ciencias, Universidad de Valladolid, E-47071 Valladolid, Spain

Received October 20, 2004

The reactions of the basal edge-bridged square-pyramidal hexanuclear cluster $[Ru_6(\mu_3\text{-}H)_2(\mu_5\text{-}\eta^2\text{-ampy})(\mu\text{-}CO)_2(CO)_{14}]$ (**1**; H_2ampy = 2-amino-6-methylpyridine) with 2 equiv of diphenylacetylene in toluene give 1 equiv of *cis*-stilbene and mixtures of cluster compounds, the composition of which depends on the reaction time and temperature. The following cluster compounds have been isolated and characterized: $[Ru_6(\mu_5\text{-}\eta^2\text{-ampy})(\mu_3\text{-}CO)(\mu\text{-}CO)_2(CO)_{14}]$ (**2**), $[Ru_6(\mu_5\text{-}\eta^2\text{-ampy})(\mu_4\text{-}\eta^2\text{-PhCCPh})(CO)_{16}]$ (**3**), $[Ru_7(\mu_5\text{-}\eta^2\text{-ampy})(\mu_5\text{-}\eta^4\text{-PhCCPh})(CO)_{17}]$ (**4**), $[Ru_6(\mu_5\text{-}\eta^2\text{-ampy})(\mu_5\text{-}\eta^8\text{-PhCCPh})(\mu\text{-}CO)(CO)_{13}]$ (**5**), $[Ru_5(\mu_5\text{-}\eta^2\text{-ampy})(\mu_4\text{-}\eta^2\text{-PhCCPh})(\mu\text{-}CO)(CO)_{12}]$ (**6**), and $[Ru_5(\mu_5\text{-}\eta^2\text{-ampy})(\mu_4\text{-}\eta^2\text{-PhCCPh})(\eta^6\text{-PhMe})(\mu\text{-}CO)(CO)_9]$ (**7**). In all products, the nitrogen atoms of the ampy ligand are attached to five metal atoms, in the same way as in complex **1**. While complex **2** has no alkyne ligand and can be considered as the result of a formal substitution of a CO ligand for the two hydrides of complex **1**, the remaining products have a diphenylacetylene ligand capping the four atoms of a metallic square through both C atoms of the original triple bond. Additionally, an alkyne phenyl group of **4** is η^2-coordinated to a ruthenium atom, while an alkyne phenyl group of **5** is η^6-coordinated to a ruthenium atom. A reaction pathway that interconnects all these compounds is proposed. This has been deduced from the results obtained by following (by ^{1}H NMR) the reaction of **1** with diphenylacetylene at different reaction times and temperatures (toluene, 80 and 110 °C), the reaction of **2** with diphenylacetylene (toluene, 110 °C), and the thermolysis of compounds **3**−**6** (toluene, 110 °C).

Introduction

The synthesis and reactivity of ruthenium carbonyl clusters derived from 2-aminopyridines have been thoroughly studied.[1,2] Most of these clusters and their derivatives are trinuclear and contain a face-capping ligand that results from the activation of an N−H bond, to give an edge-bridging amido fragment and a hydride ligand, and from the coordination of the pyridine N atom to the remaining metal atom. Some of these complexes have been recognized as catalytic precursors for the hydrogenation,[3,4] dimerization,[5] polymerization,[5] and hydroformylation[6] of selected alkynes.

The work in this field has recently led us to discover that $[Ru_3(CO)_{12}]$ can condense with triruthenium hydrido clusters of the type $[Ru_3(\mu\text{-}H)(\mu_3\text{-}\eta^2\text{-HapyR})(CO)_9]$ (H_2apyR = generic 2-aminopyridine) to give the hexanuclear derivatives $[Ru_6(\mu_3\text{-}H)_2(\mu_5\text{-}\eta^2\text{-apyR})(\mu\text{-}CO)_2(CO)_{14}]$, which have a basal edge-bridged square-pyramidal metallic skeleton.[7,8] In these compounds, five metal atoms are bridged by the N-donor ligand in such a way that the edge-bridging Ru atom is attached to the pyridine N atom, while the basal Ru atoms of the square pyramid are capped by an imido fragment that arises from the activation of both N−H bonds of the original NH_2 group (Figure 1).

Previous hexaruthenium cluster complexes with this metallic framework were very scarce, they all being

* To whom correspondence should be addressed. E-mail: jac@fq.uniovi.es. Fax: int + 34-985103446.
† Universidad de Oviedo-CSIC.
‡ Universidad de Valladolid.

(1) For a review on the reactivity of triruthenium carbonyl clusters derived from 2-aminopyridines, see: Cabeza, J. A. *Eur. J. Inorg. Chem.* **2002**, 1559.

(2) For very recent articles uncovered by the review cited in ref 1, see: (a) Cabeza, J. A.; del Río, I.; García-Granda, S.; Riera, V.; Suárez, M. *Organometallics* **2002**, *21*, 2540. (b) Cabeza, J. A.; del Río, I.; García-Granda, S.; Riera, V.; Suárez, M. *Organometallics* **2002**, *21*, 5055. (c) Cabeza, J. A.; del Río, I.; Moreno, M.; García-Granda, S.; Pérez-Priede, M.; Riera, V. *Eur. J. Inorg. Chem.* **2002**, 3204. (d) Cabeza, J. A.; del Río, I.; García-Granda, S.; Martínez-Méndez, L.; Moreno, M.; Riera, V. *Organometallics* **2003**, *22*, 1164. (e) Cabeza, J. A.; del Río, I.; García-Granda, S.; Riera, V.; Suárez, M. *Organometallics* **2004**, *23*, 3501.

(3) Cabeza, J. A. In *Metal Clusters in Chemistry*; Braunstein, P., Oro, L. A., Raithby, P. R., Eds.; Wiley-VCH: Weinheim, Germany, 1999; p 715.

(4) Cabeza, J. A.; Fernández-Colinas, J. M.; Llamazares, A. *Synlett* **1995**, 579.

(5) Nombel, P.; Lugan, N.; Mulla, F.; Lavigne, G. *Organometallics* **1994**, *13*, 4673.

(6) Nombel, P.; Lugan, N.; Donnadieu, B.; Lavigne, G. *Organometallics* **1999**, *18*, 187.

(7) Cabeza, J. A.; del Río, I.; Riera, V.; Suárez, M.; García-Granda, S. *Organometallics* **2004**, *23*, 1107.

(8) Cabeza, J. A.; del Río, I.; García-Álvarez, P.; Miguel, D.; Riera, V. *Inorg. Chem.* **2004**, *43*, 5450.

10.1021/om049186r CCC: $30.25
Publication on Web 01/15/2005

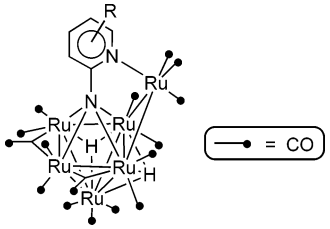

Figure 1. Schematic structure of compounds of the type $[Ru_6(\mu_3\text{-}H)_2(\mu_5\text{-}\eta^2\text{-apyR})(\mu\text{-}CO)_2(CO)_{14}]$.

byproducts of processes that generally involve various steps from $[Ru_3(CO)_{12}]$.[9−11] Their reactivity has not been studied, probably because of their low-yield preparations.

Our efficient method to synthesize these types of cluster complexes opened up the possibility of exploring their reactivity. We have recently reported the reactions of triphenylphosphine,[8] bis(diphenylphosphino)methane,[8] and [PPN][BH_4][12] with $[Ru_6(\mu_3\text{-}H)_2(\mu_5\text{-}\eta^2\text{-ampy})(\mu\text{-}CO)_2(CO)_{14}]$ (**1**; H_2ampy = 2-amino-6-methylpyridine), a complex that can be prepared in almost quantitative yield in a one-pot reaction from $[Ru_3(CO)_{12}]$ and 2-amino-6-methylpyridine.[8]

We now report the reactivity of compound **1** with diphenylacetylene. Prior to this work, the only hexaruthenium cluster complexes whose reactivity with alkynes has been examined have been compounds with octahedral metal cores.[13−15] Although some additional hexaruthenium clusters containing alkyne ligands are known, they have been prepared from precursors of lower nuclearity.[16,17]

Results and Discussion

Synthesis of Compounds 2−7. Treatment of compound **1** with 1 equiv of diphenylacetylene in refluxing toluene (110 °C) for 2 h led to a mixture of products, which contained the starting material **1** as the major component. A GC analysis of the resulting solution indicated the presence of *cis*-stilbene and the absence of diphenylacetylene.

As this suggested that more than 1 equiv of the alkyne was needed to completely consume the starting material, compound **1** was subsequently treated with 2 equiv of diphenylacetylene in refluxing toluene. After 2 h, all the starting material **1** had been consumed (IR and TLC monitoring). Again, a GC analysis of the resulting solution showed the presence of *cis*-stilbene and the absence of diphenylacetylene. A chromatographic workup allowed the isolation of the hepta-, hexa-, and pentanuclear alkyne derivatives $[Ru_7(\mu_5\text{-}\eta^2\text{-ampy})(\mu_5\text{-}\eta^4\text{-PhCCPh})(CO)_{17}]$ (**4**; 8%), $[Ru_6(\mu_5\text{-}\eta^2\text{-ampy})(\mu_5\text{-}\eta^8\text{-PhCCPh})(\mu\text{-}CO)(CO)_{13}]$ (**5**; 23%), and $[Ru_5(\mu_5\text{-}\eta^2\text{-ampy})(\mu_4\text{-}\eta^2\text{-PhCCPh})(\mu\text{-}CO)(CO)_{12}]$ (**6**; 10%) (Figure 2).

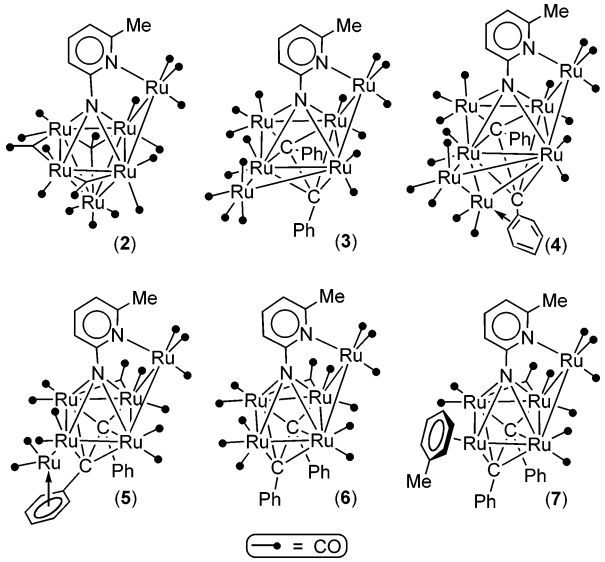

Figure 2. Schematic structures of compounds **2**−**7**.

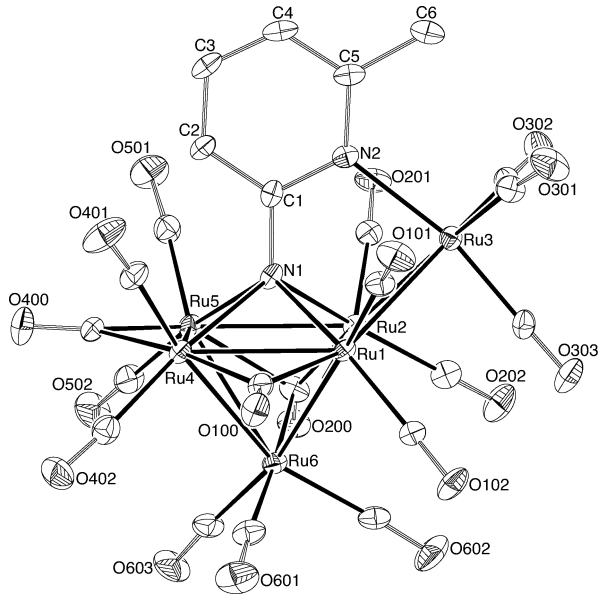

Figure 3. Molecular structure of compound **2**. For clarity, H atoms are not shown. The C and O atoms of each carbonyl ligand bear the same number.

A 24 h reaction in refluxing toluene led to a mixture from which the pentanuclear η^6-toluene derivative $[Ru_5(\mu_5\text{-}\eta^2\text{-ampy})(\mu_4\text{-}\eta^2\text{-PhCCPh})(\eta^6\text{-PhMe})(\mu\text{-}CO)(CO)_9]$ (**7**; 20%) and compounds **5** (5%) and **6** (20%) could be separated by chromatographic methods.

At 80 °C, the rate of the reaction was much slower (IR and TLC monitoring). Two intermediate hexanuclear products, $[Ru_6(\mu_5\text{-}\eta^2\text{-ampy})(\mu_3\text{-}CO)(\mu\text{-}CO)_2(CO)_{14}]$ (**2**), which contains no alkyne and no hydrides, and the alkyne derivative $[Ru_6(\mu_5\text{-}\eta^2\text{-ampy})(\mu_4\text{-}\eta^2\text{-PhCCPh})(CO)_{16}]$ (**3**), were obtained from a 14 h reaction at this temperature. These compounds were isolated by chromatographic methods in 10% and 5% yields, respectively,

(9) Chihara, T.; Tase, T.; Ogawa, H.; Wakatsuki, Y. *Chem. Commun.* **1999**, 279.
(10) Lee, K. K. H.; Wong, W. T. *J. Chem. Soc., Dalton Trans.* **1996**, 1707.
(11) (a) Adams, R. D.; Babin, J. E.; Tasi, M.; Wolfe, T. A. *J. Am. Chem. Soc.* **1988**, *110*, 7093. (b) Adams, R. D.; Babin, J. E.; Tasi, M. *Organometallics* **1988**, *7*, 503. (c) Adams, R. D.; Babin, J. E.; Tasi, M.; Wolfe, T. A. *New J. Chem.* **1988**, *12*, 481. (d) Adams, R. D.; Qu, X.; Wu, W. *Organometallics* **1994**, *13*, 1272.
(12) Cabeza, J. A.; del Río, I.; García-Álvarez, P.; Riera, V.; Suárez, M.; García-Granda, S. *Dalton* **2003**, 2808.
(13) Drake, S. R.; Johnson, B. F. G.; Lewis, J.; Conole, G.; McPartlin, M. *J. Chem. Soc., Dalton Trans.* **1990**, 995.
(14) (a) Haggitt, J. L.; Johnson, B. F. G.; Blake, A. J.; Parsons, S. J. *Chem. Commun.* **1995**, 1263. (b) Blake, A. J.; Haggitt, J. L.; Johnson, B. F. G.; Parsons, S. J. *J. Chem. Soc., Dalton Trans.* **1997**, 991.
(15) Mallors, R. L.; Blake, A. J.; Dyson, P. J.; Johnson, B. F. G. *Organometallics* **1997**, *16*, 1668.
(16) Adams, R. D.; Babin, J. E.; Tasi, M.; Wolfe, T. A. *Polyhedron* **1988**, *7*, 1071.
(17) See, for example: Lau, C. S. W.; Wong, W. T. *J. Organomet. Chem.* **1999**, *589*, 198.

Table 1. Selected Intramolecular Interatomic Distances (Å) in Compounds 2−7

	2	3	4	5	6	7
Ru(1)−Ru(2)	2.711(1)	2.704(1)	2.701(2)	2.725(4)	2.7060(6)	2.6938(9)
Ru(1)−Ru(3)	2.757(1)	2.754(1)	2.761(2)	2.727(4)	2.6820(7)	2.6797(9)
Ru(1)−Ru(4)	2.742(1)	2.774(1)	2.757(2)	2.786(4)	2.6811(7)	2.7212(9)
Ru(1)−Ru(6)	2.797(1)	2.791(1)	2.823(2)			
Ru(1)−Ru(7)			2.844(2)			
Ru(2)−Ru(3)	2.750(1)	2.692(1)	2.680(2)	2.784(5)	2.7379(7)	2.7459(9)
Ru(2)−Ru(5)	2.740(1)	2.684(1)	2.682(2)	2.726(4)	2.7099(7)	2.6959(9)
Ru(2)−Ru(6)	2.820(1)					
Ru(4)−Ru(5)	2.700(1)	2.785(1)	2.745(2)	2.846(4)	2.8011(7)	2.7546(9)
Ru(4)−Ru(6)	2.878(1)	2.751(1)	2.791(2)	2.870(4)		
Ru(4)−Ru(7)			2.833(2)			
Ru(5)−Ru(6)	2.901(2)					
Ru(6)−Ru(7)			2.601(2)			
N(1)−Ru(1)	2.148(6)	2.187(5)	2.15(1)	2.17(2)	2.151(5)	2.170(6)
N(1)−Ru(2)	2.137(6)	2.138(5)	2.22(1)	2.26(2)	2.146(5)	2.164(5)
N(1)−Ru(4)	2.254(7)	2.278(5)	2.25(1)	2.23(2)	2.211(5)	2.136(5)
N(1)−Ru(5)	2.229(7)	2.240(5)	2.22(1)	2.36(2)	2.257(5)	2.279(6)
N(2)−Ru(3)	2.221(7)	2.225(5)	2.22(1)	2.23(2)	2.220(6)	2.244(6)
C(7)−Ru(1)		2.193(6)	2.23(1)	2.33(2)	2.317(6)	2.291(7)
C(7)−Ru(2)		2.273(6)	2.24(1)			
C(7)−Ru(4)		2.386(6)	2.38(1)	2.12(2)	2.155(6)	2.080(7)
C(7)−Ru(5)				2.35(2)	2.391(6)	2.370(7)
C(7)−Ru(7)			2.61(1)			
C(8)−Ru(1)				2.29(2)	2.284(6)	2.288(7)
C(8)−Ru(2)		2.336(6)	2.33(1)	2.21(2)	2.182(7)	2.202(7)
C(8)−Ru(4)		2.356(6)	2.27(2)			
C(8)−Ru(5)		2.152(6)	2.12(1)	2.39(2)	2.341(6)	2.310(7)
C(9)−Ru(7)			2.42(1)			
C(14)−Ru(7)			2.48(1)			
C(arene)−$Ru(4)_{av}$						2.210(7)
C(arene)−$Ru(6)_{av}$				2.33(2)		

from a mixture that also afforded complex **5** (16%) and small amounts of compounds **1** and **6** that were not quantified.

As noted below, the maximum concentration of each product in the reacting solution depended on the reaction time and temperature, but we made no attempts to isolate each product in the highest possible yield.

Characterization of Compounds 2−7. These compounds were analyzed by elemental microanalysis, FAB mass spectrometry, and IR and ^{1}H NMR spectroscopy, but these techniques gave little structural information. Their molecular structures were determined by single-crystal X-ray diffraction. For comparison purposes, as far as possible, a common atom-numbering scheme has been assigned to the X-ray structures reported in this paper.

Figure 3 shows the molecular structure of compound **2**. A selection of intermolecular distances is given in Table 1. While the pyridine N atom is attached to the edge-bridging Ru atom, Ru(3), the imido N atom symmetrically caps the four basal Ru atoms. It is noteworthy that, although the plane of the ampy ligand cuts the metal framework into identical halves, the presence of the face-capping C(200)−O(200) and the edge-bridging C(100)−O(100) carbonyl ligands at either side of the ampy plane forces the complex to be asymmetric. The face-capping CO ligand is very asymmetric, the distances of its C atom to the Ru(2), Ru(5), and Ru(6) atoms being 1.99(1), 2.35(1), and 2.64(1) Å, respectively. An additional structural feature that should be highlighted is that the lengths of the four bonds that connect the apical Ru atom, Ru(6), with the basal Ru atoms are 0.1−0.2 Å longer than the remaining Ru−Ru bonds. This fact has been previously observed in other hexaruthenium complexes with this metallic skeleton.[7−13,18] Overall, this structure is reminiscent of its precursor **1**.[8] In fact, complex **2** can be considered as the result of the formal substitution of a CO ligand for the two hydrides of **1**. According to the EAN rules,[19] both **1** and **2** are electron precise, being 88-electron clusters with 10 metal−metal bonds. It is also interesting to note that all the hitherto reported hexaruthenium cluster complexes with an edge-bridged square-pyramidal metallic skeleton have an additional structural feature in common: that is, they have a ligand C-,[9] N-,[7,8,10,12] or S-donor[11] capping the basal atoms of the square pyramid. It seems that the stability of this particular hexametallic framework requires the presence of such a bridging ligand.

The molecular structure of complex **3** (Figure 4, Table 1) can be described as derived from that of complex **2**. In **3**, the Ru(6) metal atom spans the Ru(1)−Ru(4) edge. Therefore, the apical $Ru(CO)_3$ fragment of **2** has moved to an edge-bridging position in **3**. The square defined by the Ru(1), Ru(2), Ru(3), and Ru(4) atoms in **2** is now distorted toward an incipient butterfly arrangement, being capped by a diphenylacetylene ligand in such a way that the line defined by the alkyne C atoms C(7) and C(8) is almost parallel to the Ru(1)−Ru(5) vector. Consequently, it can be considered that the C atoms of the original alkyne fragment are now σ-bonded to Ru(1) and Ru(5) and π-bonded to Ru(2) and Ru(4). This type of coordination of an alkyne ligand to four metal atoms has been previously observed in many occasions, includ-

(18) Cabeza, J. A.; da Silva, I.; del Río, I.; Martínez-Méndez, L.; Miguel, D.; Riera, V. *Angew. Chem., Int. Ed.* **2004**, *43*, 3464.

(19) Mingos, D. M. P.; May, A. S. In *The Chemistry of Metal Cluster Complexes*; Shriver, D. F., Kaesz, H. D., Adams, R. D., Eds.; VCH: New York, 1990; p 11.

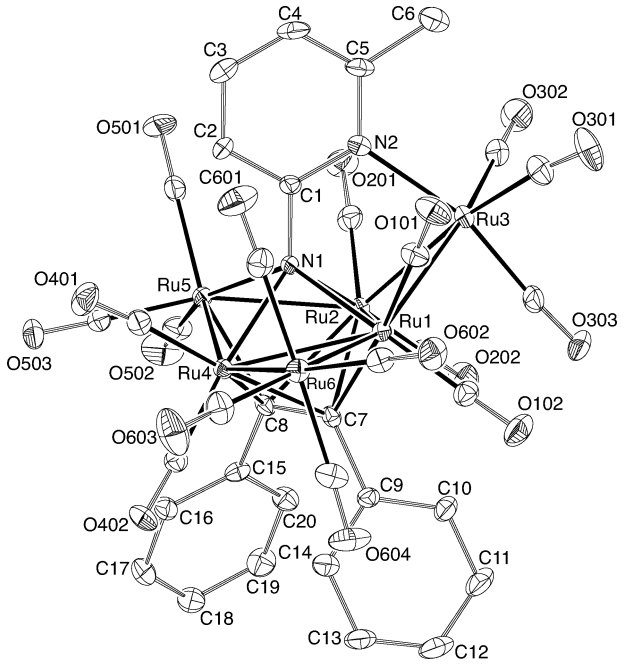

Figure 4. Molecular structure of compound **3**. For clarity, H atoms are not shown. The C and O atoms of each carbonyl ligand bear the same number.

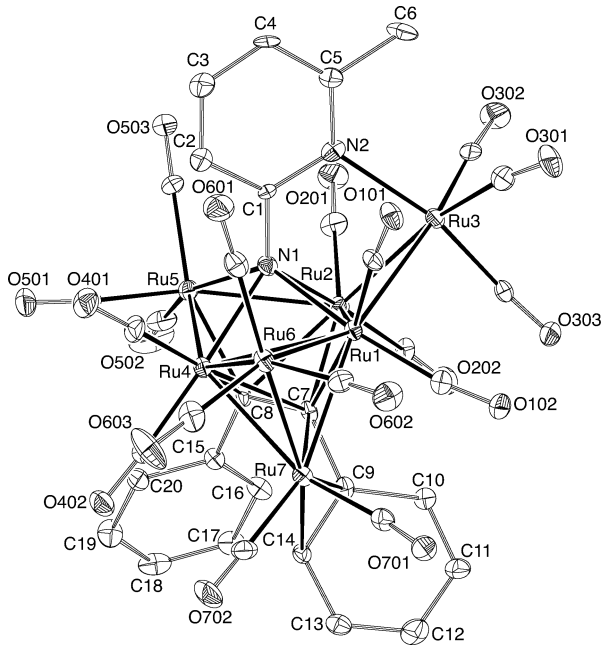

Figure 5. Molecular structure of compound **4**. For clarity, H atoms are not shown. The C and O atoms of each carbonyl ligand bear the same number.

ing some tetra-,[20−22] penta-,[20,21] and hexaruthenium[16] complexes. The cluster shell is completed with 16 terminal CO ligands. Overall, the structure of this complex is reminiscent of $[Ru_6(\mu_4\text{-}S)(\mu_4\text{-}\eta^2\text{-}PhCCH)(CO)_{17}]$, which has an analogous metallic skeleton and a similar alkyne coordination but has an S atom capping the metallic square.[16]

Compound **4** is heptanuclear. Its molecular structure (Figure 5, Table 1) can be described from that of complex **3**. The additional metal atom, Ru(7), caps the Ru(1)−Ru(4)−Ru(6) triangle, forming a tetrahedron that shares the Ru(1)−Ru(4) edge with the distorted square capped by the imido N atom. As in **3**, the C(7) and C(8) atoms of the alkyne fragment of **4** cap the four metal atoms of the distorted square, but additionally, two C atoms of a phenyl group, C(9) and C(14), are coordinated to Ru(7). The C(7)−Ru(7) distance, 2.61(1) Å, is short enough to be considered a bonding interaction. The cluster shell is completed with 17 terminal CO ligands.

Compound **5** is hexanuclear. Its molecular structure (Figure 6, Table 1) can also be described from that of complex **3**. In this case, the Ru(6) atom is attached to one metal atom only, Ru(4), and one of the phenyl groups is η^6-coordinated to Ru(6). A small rotation of the alkyne has now placed the C(7)−C(8) bond in a parallel position to the Ru(2)−Ru(4) vector, the alkyne being σ-bonded to Ru(2) and Ru(4) and π-bonded to Ru(1) and Ru(5). The cluster shell is completed with 13 terminal and 1 bridging CO ligand. Although the coordination of arenes to ruthenium carbonyl clusters as η^6 ligands is now well established,[23] the coordination of diphenylacetylene as an η^8 ligand is unprecedented.

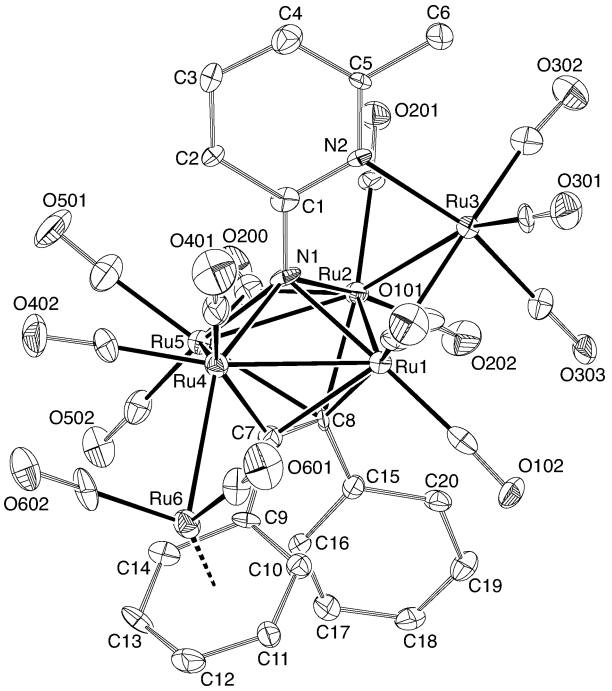

Figure 6. Molecular structure of compound **5**. For clarity, H atoms are not shown. The C and O atoms of each carbonyl ligand bear the same number.

(20) Adams, R. D.; Babin, J. E.; Tasi, M.; Wolfe, T. A. *Organometallics* **1987**, *6*, 2228.

(21) Ho, E. N. M.; Wong, W. T. *J. Chem. Soc., Dalton Trans.* **1998**, 4215.

(22) See, for example: (a) Blohm, M. L.; Gladfelter, W. L. *Organometallics* **1986**, *5*, 1049. (b) Ho, E. N. M.; Wong, W. T. *J. Chem. Soc., Dalton Trans.* **1998**, 513. (c) Ho, E. N. M.; Lin, Z.; Wong, W. T. *Eur. J. Inorg. Chem.* **2001**, 1321. (d) Cabeza, J. A.; del Río, I.; García-Granda, S.; Moreno, M.; Riera, V.; Rosales-Hoz, M. J.; Suárez, M. *Eur. J. Inorg. Chem.* **2001**, 2899. (e) Corrigan, J. F.; Doherty, S.; Taylor, N. J.; Carty, A. J. *Organometallics* **1985**, *4*, 2066. (f) Corrigan, J. F.; Doherty, S.; Taylor, N. J.; Carty, A. J. *Organometallics* **1993**, *12*, 1365. (g) Jackson, P. F.; Johnson, B. F. G.; Lewis, J.; Raithby, P. *J. Chem. Soc., Chem. Commun.* **1980**, 1190. (h) Braga, D.; Grepioni, F.; Brown, D. B.; Johnson, B. F. G.; Calhorda, M. J. *Organometallics* **1996**, *15*, 5723. (i) Deeming, A. J.; Speel, D. M. *Organometallics* **1997**, *16*, 289. (j) Bruce, M. I.; Zaitseva, N. N.; Skelton, B. W.; White, A. H. *Dalton* **2002**, 3879. (k) Bruce, M. I.; Skelton, B. W.; White, A. H.; Zaitseva, N. N. *Aust. J. Chem.* **1999**, *52*, 681.

(23) For a review on η^6-arene ruthenium clusters, see: Braga, D.; Dyson, P. J.; Grepioni, F.; Johnson, B. F. G. *Chem. Rev.* **1994**, *94*, 1585.

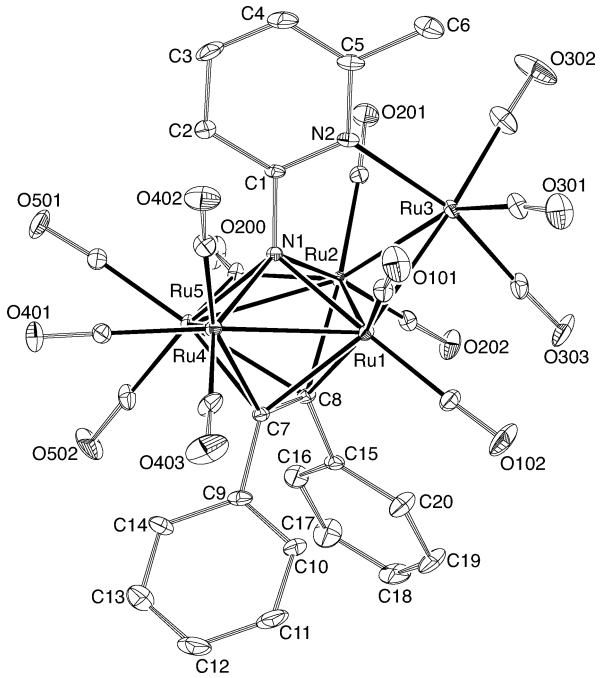

Figure 7. Molecular structure of compound **6**. For clarity, H atoms are not shown. The C and O atoms of each carbonyl ligand bear the same number.

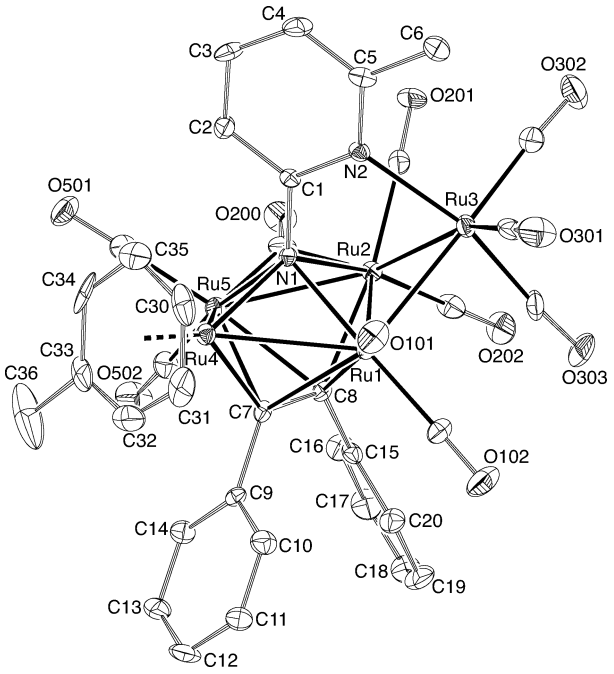

Figure 8. Molecular structure of compound **7**. For clarity, H atoms are not shown. The C and O atoms of each carbonyl ligand bear the same number.

Compound **6** is pentanuclear. Its molecular structure (Figure 7, Table 1) can be described as resulting from the formal replacement of a carbonyl ligand for the arene-coordinated $Ru(CO)_2$ fragment of complex **5**. The cluster contains 12 terminal CO ligands and 1 bridging CO ligand. This structure is reminiscent of $[Ru_5(\mu_4\text{-S})(\mu_4\text{-}\eta^2\text{-PhCCH})(\mu\text{-CO})(CO)_{13}]$[16,20] and $[Ru_5(\mu_4\text{-NH})(\mu_4\text{-}\eta^2\text{-PhCCH})(\mu\text{-CO})(CO)_{13}]$.[21] These complexes and compound **6** have in common their metallic skeletons and the way the alkyne coordinates to the metals but differ in the nature of the ligand that caps the metallic square.

Compound **7** is also pentanuclear. Its molecular structure (Figure 8, Table 1) can be described as resulting from the formal replacement of an η^6-toluene ligand for the three CO ligands attached to the Ru(4) atom of complex **6**, the remaining atoms maintaining the same positions as in **6**. Quite a few carbonyl ruthenium clusters containing terminal η^6-arene ligands are already known.[23]

^{1}H NMR Monitoring of the Reactions. The ampy methyl group was a convenient label that made it easy to recognize and quantify the presence of each product in the reaction mixtures. Fortunately, the ^{1}H NMR spectra of all these complexes display the resonance of the methyl group of each complex at a distinctive chemical shift. This fact permitted the monitoring of the reactions, which was performed by analyzing the ^{1}H NMR spectra of the residues obtained after removing the solvent of aliquots taken from the reacting solutions at different reaction times.

Figure 9 shows the evolution of the reaction of **1** with 2 equiv of diphenylacetylene at 110 °C over a period of 24 h. Three species were observed at the initial stages of the reaction (5 min), complexes **2** and **3** and a new species, hereafter labeled as **3a**, which was characterized by a singlet at 2.68 ppm in the ^{1}H NMR ($CDCl_3$) of the reaction mixtures. The spectrum corresponding to $t = 15$ min showed an increase of the concentration of **2** and the appearance of complexes **4**−**6**. In the 15−45 min period, the consumption of the starting material **1** was accompanied by an increase of the concentration of **5** (33%), while the amount of each of the remaining complexes varied very little. In the 45−180 min period, the concentrations of **5** (63%) and **6** (32%) increased noticeably. A small amount of complex **4** (5%) was still present at $t = 180$ min, while **2**, **3**, and **3a** were missing. Compound **7** was first observed at $t = 7$ h. Its concentration increased slowly with time, becoming the major product at $t = 24$ h (44%), while a considerable amount of complex **6** (42%) and a small amount of complex **5** (14%) were still present in the solution.

As we had noticed that at 80 °C the reaction was much slower than at 110 °C, we decided to follow it by ^{1}H NMR spectroscopy in order to know the behavior of the intermediate species **2**, **3**, **3a**, and **4** at this temperature (at 110 °C, these species, when present, were always in low concentrations). The reaction was monitored for 22 h. What is shown in Figure 10 is somehow comparable to the 5−45 min period of Figure 9, but there are noticeable differences: (a) at 80 °C, the heptanuclear complex **4** was never observed, (b) the concentration of complex **2** in the 15−45 min period at 110 °C is higher than in the 2−22 h period at 80 °C, and (c) the concentrations of **3** and **3a** in the 15−45 min period at 110 °C are lower than in the 2−22 h period at 80 °C.

As complex **2**, which contains no alkyne ligand, seemed to be an early intermediate in the reactions, the reaction of this complex with 1 equiv of diphenylacetylene at 110 °C was also monitored by ^{1}H NMR. The results (see the Experimental Section) were comparable to those obtained by starting from **1** and 2 equiv of diphenylacetylene.

All attempts (TLC, column chromatography) to separate complex **3a** from the mixtures were unsuccessful.

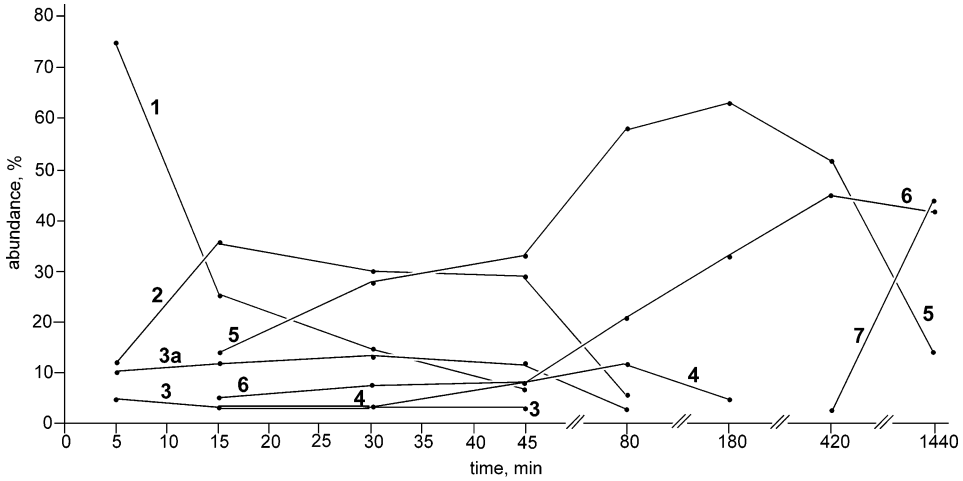

Figure 9. ^{1}H NMR monitoring of the reaction of complex **1** with 2 equiv of diphenylacetylene at 110 °C.

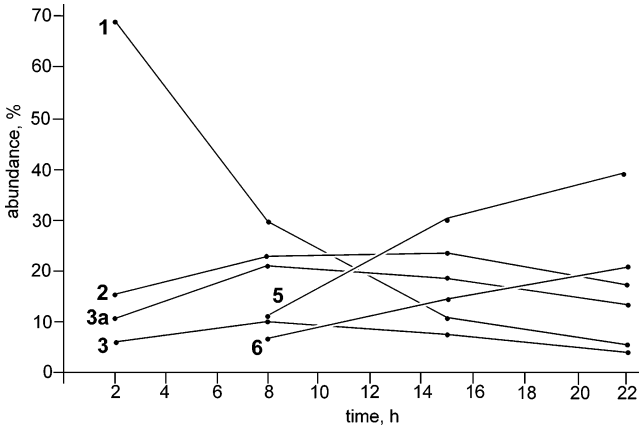

Figure 10. ^{1}H NMR monitoring of the reaction of complex **1** with 2 equiv of diphenylacetylene at 80 °C.

It always decomposed on the chromatographic supports (silica gel, alumina).

Thermolysis of Compounds 3−6. With the objective to gain a deeper insight into the relationships between the compounds involved in the transformation of complex **1** into complex **7**, we studied the individual thermolysis of compounds **3**−**6** in refluxing toluene (^{1}H NMR monitoring).

The thermolysis of complex **3** gave, after 5 min, a mixture of **3a** (46%), **4** (3%), **5** (40%), and **6** (11%). After 30 min, **3** and **3a** were absent and compounds **5** (82%) and **6** (16%) were accompanied by a very small amount of complex **4** (2%). It seems that complexes **4** and **5** are formed from **3** and/or **3a** at different rates, the formation of **4** being much slower than that of **5**. The short life of complexes **3** and **3a** and the slow formation of **4** explain why, in the reaction of **1** with diphenylacetylene, these species are present always in low concentrations. The results of this thermolytic reaction confirmed that complex **2**, which was unobserved at any stage of the thermolysis, does not arise from complex **3**. They also indicated that complex **4** has a much longer life than **3** and **3a** in refluxing toluene.

In fact, the thermolysis of complex **4** was slow. After 50 min, most of this compound remained unreacted, being accompanied by complexes **5** (34%) and **6** (10%). This reaction also confirmed that **4** is not a precursor of **3** and **3a**.

The individual thermolysis of compounds **5** and **6** in refluxing toluene indicated that both complexes are interrelated by a chemical equilibrium, since each of them was observed as a product when the other was subjected to thermolysis. These reactions also confirmed that complex **7** arises from a slow reaction of **6** with toluene.

Reaction Pathway. All the aforementioned data allowed us to propose a reasonable reaction pathway for the conversion of complex **1** into complex **7**. Such a proposal is shown in Scheme 1.

As none of the observed products contain hydride ligands, as 2 equiv of diphenylacetylene is necessary to observe the complete consumption of complex **1**, and as uncoordinated *cis*-stilbene is observed in the reaction solution from its initial stages, we propose that the first equivalent of the alkyne reacts with **1** to form (in various steps that would also involve the release and recoordination of CO) a very unstable species, which has not been detected, containing *cis*-stilbene as a ligand (**1a** in Scheme 1). These species would rapidly evolve through two different pathways that imply the elimination of *cis*-stibene and the incorporation of CO, to give **2**, or diphenylacetylene, to give **3**. We believe that **3** should be more rapidly formed than **2** because the concentration of diphenylacetylene in solution should be much higher than that of CO at the initial stages of the reaction (the latter arises from subsequent processes). However, complex **2** was always present in solution in a greater amount than **3**, despite the fact that it also reacts with diphenylacetylene to give **3**. This was explained by the results of the reaction of **2** with diphenylacetylene and the individual thermolysis of complex **3**, which indicated that, at 110 °C, **3** evolves in solution toward other products more quickly than **2** reacts with diphenylacetylene to give **3**. In any case, the formation of **3** from **1a** and **2** implies that, upon coordination of diphenylacetylene, the apical Ru atom is displaced to an edge-bridging position.

The results obtained from the thermolysis of **3** indicated that **3a** is a short-lived intermediate and that complex **5** is formed more rapidly than the heptanuclear derivative **4**. Complex **4** slowly decomposed to give **5** but not **3** or **3a**. The thermolysis of **5** gave **6** but not **3**, **3a**, or **4**, and the thermolysis of **6** gave some **5** and the η^6-toluene derivative **7**. These data indicate that complex

Scheme 1. Reaction Pathway for the Transformation of Complex 1 into Complex 7

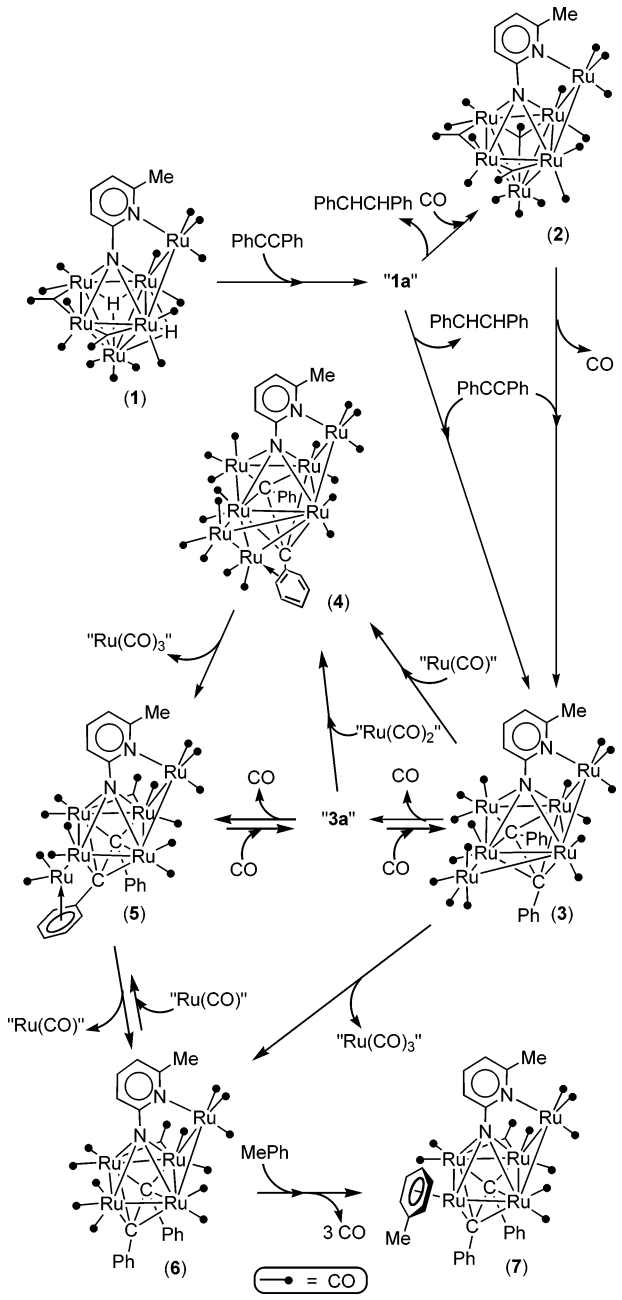

4 is irreversibly formed from **3** and/or **3a**, that most of complex **5** should arise from a CO loss from **3a** because the transformation of **4** into **5** is slow, and that the transformation of **5** into **6** is slow and reversible, this equilibrium being displaced toward complex **6**.

Complex **3a** has not been isolated, but it has been detected in the reaction mixtures by ^{1}H NMR spectroscopy. Although its structure remains unknown, from the structures of compounds **4** and **5**, it can be presumed that **3a** has one CO ligand less than **3** and that one of its phenyl groups interacts with the edge-bridging metal atoms in a way analogous to that found in complex **4**.

The transformation of **3** into **5** is a reversible process. This was checked by slowly bubbling carbon monoxide through a toluene solution of complex **5** at 80 °C for 2 h, which led to a solution containing **3** (70%), **5** (6%), and **6** (24%). These data were obtained by integration of the ^{1}H NMR spectrum of the crude solid obtained after solvent removal.

Some complex **6** may also be formed directly from **3**. However, we believe that the extent of this process should be very small because, prior to the disappearance of complex **3**, the concentration of **6** in the reacting solution is very small (Figure 9), starting to increase after a considerable amount of complex **5** has already been accumulated in the reacting solution (the transformation of **5** into **6** is slow). In other words, the transformation of **3** into **5** should be much faster than the direct transformation of **3** into **6**.

Some steps shown in Scheme 1 involve the exchange of $Ru(CO)_n$ fragments between clusters. Such processes are not unusual when working with ruthenium carbonyl clusters at high temperatures.[11b,16,18,20] For example, a cluster growth/reduction sequence, similar to that described herein for the hepta-, hexa-, and pentanuclear compounds **4**−**6**, was observed to occur for the cluster series $[Ru_7(\mu_4\text{-}S)(CO)_{21}]$, $[Ru_6(\mu_4\text{-}S)(CO)_{18}]$, and $[Ru_5(\mu_4\text{-}S)(CO)_{15}]$.[11b]

Concluding Remarks

The present work is the first reactivity study involving hexaruthenium cluster complexes of basal edge-bridged square pyramidal metallic skeleton and unsaturated organic molecules. The reaction of compound **1** with diphenylacetylene is complicated, because it involves a considerable number of intermediates and side products. Nevertheless, a nearly complete picture of the whole process has been obtained (Scheme 1). Six products, including penta-, hexa-, and heptanuclear alkyne derivatives, have been characterized by X-ray diffraction methods and the chemical relationships between them have been established.

Without exception, the alkyne prefers to cap a (distorted) square of metal atoms rather than to coordinate to a triangular metal face, even though, in some cases, this process requires the displacement of the metal atom that originally occupied such a site toward an edge-bridging position.

From this work, it is evident that the ampy ligand behaves as a useful label to trace the intermediates and reaction products by ^{1}H NMR spectroscopy, behaving also as a reliable anchor that is able not only to maintain the pentanuclear edge-bridged square metal framework in reactions performed at high temperatures (<110 °C) but also to avoid the participation of these metal atoms in metal exchange processes between clusters.

Experimental Section

General Data. Solvents were dried over sodium diphenyl ketyl (hydrocarbons, THF) or CaH_2 (dichloromethane) and distilled under nitrogen prior to use. The reactions were carried out under nitrogen, using Schlenk−vacuum line techniques, and were routinely monitored by solution IR spectroscopy (carbonyl stretching region) and spot TLC. Compound **1** was prepared as previously reported.[8] IR spectra were recorded in solution on a Perkin-Elmer Paragon 1000 FT spectrophotometer. ^{1}H NMR spectra were run on a Bruker DPX-300 instrument, at room temperature, using the dichloromethane solvent resonance as internal standard (δ 5.30). Microanalyses were obtained from the University of Oviedo

Analytical Service. FAB-MS were obtained from the University of Santiago de Compostela Mass Spectrometric Service; data given refer to the most abundant molecular ion isotopomer.

Reactions of Compound 1 with Diphenylacetylene. Reaction a. A solution of **1** (100 mg, 0.086 mmol) and diphenylacetylene (31 mg, 0.172 mmol) in toluene (20 mL) was heated at reflux temperature for 2 h. The color changed from dark brown to dark orange-brown. The solvent was removed under reduced pressure, and the residue was dissolved in dichloromethane (10 mL). After silica gel was added (ca. 3 g), the solvent was evaporated under reduced pressure and the solid residue was placed onto a silica gel column (2 × 20 cm) packed in hexane. Hexane−diethyl ether (20:1) eluted a dark brown band containing a mixture of compounds **4** and **6**. Hexane−diethyl ether (5:1) eluted a weak green band containing a small amount of complex **6** and other unidentified products. Hexane−dichloromethane (2:1) eluted an orange band, which afforded compound **5** as a dark orange solid after solvent removal (25 mg, 23%). A black residue remained uneluted at the top of the column. The solution containing the first band (dark brown) was evaporated to dryness, the solid residue was dissolved in THF (1 mL), and the extract was subjected to a TLC separation (silica gel), using hexane−diethyl ether (1:1) as eluant. Extraction of the first band (dark brown) with dichloromethane allowed the isolation of complex **4** (8 mg, 7%). Extraction of the second band (orange-brown) allowed the isolation of complex **6** (10 mg, 10%).

Reaction b. A solution of **1** (100 mg, 0.086 mmol) and diphenylacetylene (31 mg, 0.172 mmol) in toluene (20 mL) was heated at reflux temperature for 24 h. The original dark brown color acquired a greenish orange tone. The solvent was removed under reduced pressure, and the residue was dissolved in dichloromethane (10 mL). After silica gel was added (ca. 3 g), the solvent was evaporated under reduced pressure and the solid residue was placed onto a silica gel column (2 × 20 cm) packed in hexane. Hexane−dichloromethane (10:1) eluted a very small amount of a yellow unidentified compound. Hexane−dichloromethane (5:1) eluted two bands. The fastest moving band, orange-brown, afforded compound **6** as a dark orange-brown solid after solvent removal (20 mg, 20%). The following band, pink, contained a very small amount of an unidentified product. Hexane−dichloromethane (3:1) eluted a dark green band, which afforded compound **7** as a dark green solid after solvent removal (20 mg, 20%). Subsequent elution with hexane−dichloromethane (1:1) eluted the orange complex **5** (6 mg, 5%). A black residue remained uneluted at the top of the column.

Reaction c. A solution of **1** (100 mg, 0.086 mmol) and diphenylacetylene (31 mg, 0.172 mmol) in toluene (20 mL) was heated at 80 °C for 14 h. The original dark brown color acquired a greenish orange tone. The solvent was removed under reduced pressure, and the residue was dissolved in dichloromethane (10 mL). After silica gel was added (ca. 3 g), the solvent was evaporated under reduced pressure and the solid residue was placed onto of a silica gel column (2 × 25 cm) packed in hexane. Hexane−diethyl ether (8:1) eluted a dark green band that contained a small amount of compound **3** (5 mg, 4%). Hexane−diethyl ether (5:1) eluted an orange-brown band that contained a mixture of compounds **1**, **3**, and **6**. Hexane−dichloromethane (5:1) eluted a trace amount of an unidentified pink complex. Hexane−dichloromethane (3:1) eluted a dark green band that contained compound **2** (10 mg, 10%). Hexane−dichloromethane (1:1) eluted an orange band that afforded compound **5** as a dark orange solid after solvent removal (18 mg, 16%). A black residue remained uneluted at the top of the column.

^{1}H NMR Monitoring of the Reactions. This was carried out by analyzing the ^{1}H NMR spectra ($CDCl_3$ solution) of the solid residues obtained after removing the solvent of 0.3 mL aliquots taken from the reacting solutions at different reaction times. In the following paragraphs, the figure given in parentheses just after the compound number corresponds to the approximate percentage of that compound in the solution. Only soluble complexes containing the ampy ligand were taken into account to calculate the percentages, because they were elaborated from the ^{1}H NMR integrals of the resonances of the ampy ligand methyl groups.

(a) Reaction of Compound 1 with Diphenylacetylene at 110 °C. A solution of compound **1** (100 mg, 0.086 mmol) and diphenylacetylene (31 mg, 0.172 mmol) in toluene (20 mL) was stirred at reflux temperature. ^{1}H NMR monitoring: (a) after 5 min **1** (74), **2** (12), **3** (4), and **3a** (10); (b) after 15 min **1** (26), **2** (37), **3** (3), **3a** (12), **4** (3), **5** (14), and **6** (5); (c) after 30 min **1** (13), **2** (27), **3** (4), **3a** (13), **4** (4), **5** (28), and **6** (11); (d) after 45 min **1** (5), **2** (28), **3** (3), **3a** (9), **4** (5), **5** (33), and **6** (8); (e) after 80 min **2** (6), **3a** (3), **4** (12), **5** (58), and **6** (21); (f) after 3 h **4** (5), **5** (63), and **6** (32); (g) after 7 h **5** (52), **6** (45), and **7** (3); (h) after 24 h **5** (14), **6** (42), and **7** (44).

(b) Reaction of Compound 1 with Diphenylacetylene at 80 °C. A solution of compound **1** (100 mg, 0.086 mmol) and diphenylacetylene (31 mg, 0.172 mmol) in toluene (20 mL) was stirred at reflux temperature. ^{1}H NMR monitoring: (a) after 2 h **1** (68), **2** (15), **3** (6), and **3a** (11); (b) after 8 h **1** (30), **2** (23), **3** (10), **3a** (21), **5** (10), and **6** (6); (c) after 15 h **1** (11), **2** (20), **3** (7), **3a** (18), **5** (29), and **6** (15); (d) after 22 h **1** (5), **2** (19), **3** (4), **3a** (13), **5** (38), and **6** (20).

(c) Reaction of Compound 2 with Diphenylacetylene at 110 °C. A solution of compound **2** (10 mg, 0.008 mmol) and diphenylacetylene (2 mg, 0.011 mmol) in toluene (8 mL) was stirred at 80 °C. ^{1}H NMR monitoring: (a) after 20 min **2** (61), **3** (2), **3a** (12), **5** (20), and **6** (5); (b) after 50 min **2** (27), **3a** (6), **4** (3), **5** (49), and **6** (15); (c) after 2 h **3a** (5), **4** (6), **5** (67), and **6** (22).

(d) Thermolysis of Compound 3 at 110 °C. Compound **3** (5 mg, 0.004 mmol) in toluene (6 mL) was stirred at reflux temperature. ^{1}H NMR monitoring: (a) after 5 min **3a** (46), **4** (3), **5** (40), and **6** (11); (b) after 30 min **4** (2) **5** (80) and **6** (18).

(e) Thermolysis of Compound 4 at 110 °C. Compound **4** (3 mg, 0.002 mmol) was heated in toluene (3 mL) at reflux temperature for 50 min. The solution was evaporated to dryness, and the residue was analyzed by ^{1}H NMR spectroscopy: **4** (56), **5** (34), and **6** (10).

(f) Thermolysis of Compound 5 at 110 °C. Compound **5** (15 mg, 0.012 mmol) was heated in toluene (10 mL) at reflux temperature for 8 h. The solution was evaporated to dryness, and the residue was analyzed by ^{1}H NMR spectroscopy: **5** (39), **6** (34), and **7** (27).

(g) Thermolysis of Compound 6 at 110 °C. Compound **6** (12 mg, 0.010 mmol) was heated in toluene (8 mL) at reflux temperature for 15 h. The solution was evaporated to dryness, and the residue was analyzed by ^{1}H NMR spectroscopy: **5** (9), **6** (16), and **7** (75).

Data for [$Ru_6(\mu_5\text{-}\eta^2\text{-ampy})(\mu_3\text{-CO})(\mu\text{-CO})_2(CO)_{14}$] (2). Anal. Calcd for $C_{23}H_6N_2O_{17}Ru_6$ (fw = 1188.72): C, 23.24; H, 0.51; N, 2.36. Found: C, 23.21; H, 0.56; N, 2.31. Positive FAB MS: *m/z* 1189 [M^+]. IR (CH_2Cl_2): ν(CO) 2094 (w), 2065 (s), 2040 (s), 2013 (m), 1993 (w, sh), 1975 (vw, sh), 1854 (w, br), 1823 (w, br) cm^{-1}. ^{1}H NMR ($CDCl_3$): δ 7.21 (t, J = 8.0 Hz, 1 H, ampy), 6.61 (d, J = 8.0 Hz, 1 H, ampy), 6.03 (d, J = 8.0 Hz, 1 H, ampy), 2.36 (s, 3 H, ampy).

Data for [$Ru_6(\mu_5\text{-}\eta^2\text{-ampy})(\mu_4\text{-}\eta^2\text{-PhCCPh})(CO)_{16}$] (3). Anal. Calcd for $C_{36}H_{16}N_2O_{16}Ru_6$ (fw = 1338.94): C, 32.29; H, 1.20; N, 2.09. Found: C, 32.19; H, 1.17; N, 2.12. Positive FAB MS: *m/z* 1312 [$(M - CO)^+$]. IR (CH_2Cl_2): ν(CO) 2105 (m), 2071 (vs), 2058 (vs), 2033 (s), 2023 (s), 2000 (vs, br), 1972 (w, br), 1934 (m, br) cm^{-1}. ^{1}H NMR (CD_2Cl_2): δ 7.86 (d, br, J = 7.5 Hz, 1 H, Ph), 7.33 (t, J = 7.7 Hz, 1 H, ampy), 7.26 (td, J = 7.5, 1.2 Hz, 1 H, Ph), 7.2−7.1 (m, 2 H, Ph), 6.88 (tt, J = 7.5, 1.1 Hz, 1 H, Ph), 6.76 (tt, J = 7.5, 1.4 Hz, 1 H, Ph), 6.70 (d, J = 7.7 Hz, 1 H, ampy), 6.6−6.5 (m, 2 H, Ph), 6.47 (d, J = 7.7 Hz, 1 H, ampy), 5.87 (d, br, J = 7.5 Hz, 1 H, Ph), 5.60 (d, br, J = 7.5 Hz, 1 H, Ph), 2.66 (s, 3 H, ampy).

Table 2. Crystal, Measurement, and Refinement Data for the Compounds Studied by X-ray Diffraction

	2·0.5CH_2Cl_2	**3**	**4**·0.75CH_2Cl_2	**5**·0.4CH_2Cl_2	**6**	**7**
formula	$C_{23}H_7N_2O_{17}Ru_6$·0.5CH_2Cl_2	$C_{36}H_{16}N_2O_{16}Ru_6$	$C_{37}H_{16}N_2O_{17}Ru_7$·0.75$CH_2Cl_2$	$C_{34}H_{16}N_2O_{14}Ru_6$·0.4$CH_2Cl_2$	$C_{33}H_{16}N_2O_{13}Ru_5$	$C_{37}H_{24}N_2O_{10}Ru_5$
formula wt	1232.19	1338.93	1530.19	1316.88	1153.83	1161.93
cryst syst	monoclinic	orthorhombic	monoclinic	monoclinic	orthorhombic	orthorhombic
space group	*C*2/*c*	$P2_12_12_1$	*C*2/*c*	$P2_1/n$	$P2_12_12_1$	*Pbca*
a, Å	32.396(13)	12.354(5)	21.6445(3)	15.17(3)	11.1372(2)	19.296(3)
b, Å	11.514(5)	17.951(7)	11.3872(1)	12.55(2)	16.4202(3)	17.896(3)
c, Å	18.087(7)	18.506(7)	70.7952(7)	23.20(4)	19.2955(3)	21.224(4)
β, deg	104.201(7)	90	92.101(1)	92.75(3)	90	90
V, Å^3	6540(4)	4104(3)	17437.2(3)	4412(13)	3528.7(1)	7329(2)
Z	8	4	16	4	4	8
F(000)	4640	2552	11616	2507	2208	4480
D_{calcd}, g cm^{-3}	2.503	2.167	2.332	1.983	2.172	2.106
radiation (λ, Å)	Mo Kα (0.710 73)	Mo Kα (0.710 73)	Cu Kα (1.541 80)	Mo Kα (0.710 73)	Cu Kα (1.541 80)	Mo Kα (0.710 73)
μ, mm^{-1}	2.860	2.225	20.625	2.111	17.545	2.075
cryst size, mm	0.15 × 0.23 × 0.29	0.12 × 0.27 × 0.36	0.18 × 0.10 × 0.08	0.05 × 0.15 × 0.37	0.13 × 0.10 × 0.10	0.11 × 0.27 × 0.29
temp, K	296(2)	296(2)	200(2)	299(2)	293(2)	296(2)
θ limits, deg	1.88−23.26	1.58−23.27	1.25−68.21	1.57−24.05	3.53−70.07	1.82−23.28
min/max *h*, *k*, *l*	−35 to +35, −9 to +12, −20 to +19	−13 to +13, −19 to +19, −20 to +14	−26 to +26, 0−13, 0−85	−16 to +17, −9 to +14, −23 to +25	0−13, 0−19, 0−23	−21 to +20, −19 to +18, −23 to +16
no. of collected rflns	14 139	18 318	43 305	18 473	9809	30 526
no. of unique rflns	4672	5898	15 768	6387	3719	5254
no. of rflns with $I > 2\sigma(I)$	4077	5616	11 037	4365	3684	4543
abs cor	SADABS	SADABS	SORTAV	SADABS	SORTAV	SADABS
max/min transmissn	1.000/0.725	1.000/0.700	0.215/0.130	1.000/0.980	0.175/0.167	1.000/0.720
no. of params/ restraints	462/0	542/0	1188/5	480/0	479/0	489/0
GOF on F^2	1.208	1.171	1.001	1.109	1.188	1.220
R1 (on F, $I > 2\sigma(I)$)	0.0397	0.0253	0.0781	0.1022	0.0251	0.0439
wR2 (on F^2, all data)	0.0881	0.0606	0.2350	0.2558	0.0665	0.0909
max/min $\Delta\rho$, e Å^{-3}	1.150/−0.740	0.510/−0.528	2.414/−2.399	1.988/−2.226	0.648/−1.045	0.701/−0.922

Data for [$Ru_7(\mu_5\text{-}\eta^2\text{-ampy})(\mu_5\text{-}\eta^4\text{-PhCCPh})(CO)_{17}$] (4). Anal. Calcd for $C_{37}H_{16}N_2O_{17}Ru_7$ (fw = 1468.02): C, 30.27; H, 1.10; N, 1.91. Found: C, 30.20; H, 1.05; N, 1.82. Positive FAB MS: *m/z* 1384 [(M − 3CO)$^+$]. IR (CH_2Cl_2): ν(CO) 2080 (w), 2060 (vs), 2032 (w, sh), 2008 (s, br), 1979 (w, sh), 1930 (w, br) cm^{-1}. ^{1}H NMR ($CDCl_3$): δ 7.77 (d, br, J = 7.6 Hz, 1 H, Ph), 7.39 (t, J = 7.6 Hz, 1 H, Ph), 7.32 (t, J = 7.8 Hz, 1 H, ampy), 7.11 (t, J = 7.4 Hz, 1 H, Ph), 7.05 (t, J = 7.6 Hz, 1 H, Ph), 7.0−6.9 (m, 2 H, Ph), 6.77 (t, J = 7.4 Hz, 1 H, Ph), 6.71 (d, J = 7.8 Hz, 1 H, ampy), 6.58 (t, J = 7.4 Hz, 1 H, Ph), 6.11 (d, J = 7.8 Hz, 1 H, ampy), 5.46 (d, br, J = 7.4 Hz, 1 H, Ph), 4.79 (d, br, J = 7.6 Hz, 1 H, Ph), 2.73 (s, 3 H, ampy).

Data for [$Ru_6(\mu_5\text{-}\eta^2\text{-ampy})(\mu_5\text{-}\eta^8\text{-PhCCPh})(\mu\text{-CO})(CO)_{13}$] (5). Anal. Calcd for $C_{34}H_{16}N_2O_{14}Ru_6$ (fw = 1282.92): C, 31.83; H, 1.26; N, 2.18. Found: C, 31.78; H, 1.22; N, 2.17. Positive FAB MS: *m/z* 1284 [M$^+$]. IR (CH_2Cl_2): ν(CO) 2066 (m), 2039 (s), 2023 (vs), 2008 (m), 1995 (m, br), 1985 (m, sh), 1962 (m, br), 1928 (w, br), 1915 (w, br), 1827 (w, br) cm^{-1}. ^{1}H NMR (CD_2Cl_2): δ 7.16 (t, J = 7.8 Hz, 1 H, ampy), 7.1−7.0 (m, 3 H, Ph), 6.9−6.8 (m, 3 H, Ph), 6.53 (d, J = 7.8 Hz, 1 H, ampy), 6.23 (t, J = 6.7 Hz, 1 H, Ph), 6.16 (d, J = 7.8 Hz, 1 H, ampy), 5.90 (t, J = 6.7 Hz, 1 H, Ph), 5.07 (d, br, J = 6.7 Hz, 1 H, Ph), 4.04 (d, br, J = 6.7 Hz, 1 H, Ph), 2.57 (s, 3 H, ampy).

Data for [$Ru_5(\mu_5\text{-}\eta^2\text{-ampy})(\mu_4\text{-}\eta^2\text{-PhCCPh})(\mu\text{-CO})(CO)_{12}$] (6). Anal. Calcd for $C_{33}H_{16}N_2O_{13}Ru_5$ (fw = 1153.84): C, 34.35; H, 1.40; N, 2.43. Found: C, 34.20; H, 1.38; N, 2.40. Positive FAB MS: *m/z* 1155 [M$^+$]. IR (CH_2Cl_2): ν(CO) 2082 (w), 2060 (vs), 2032 (vs), 2018 (s), 2005 (s), 1978 (m, sh), 1973 (m, br), 1936 (w, br), 1837 (w, br) cm^{-1}. ^{1}H NMR ($CDCl_3$): δ 7.12 (t, J = 8.0 Hz, 1 H, ampy), 7.0−6.9 (m, 3 H, Ph), 6.8−6.6 (m, 5 H, Ph), 6.56 (d, J = 8.0 Hz, 1 H, ampy), 5.90 (m, 1 H, Ph), 5.67 (d, J = 8.0 Hz, 1 H, ampy), 5.62 (d, J = 7.6 Hz, 1 H, Ph), 2.62 (s, 3 H, ampy).

Data for [$Ru_5(\mu_5\text{-}\eta^2\text{-ampy})(\mu_4\text{-}\eta^2\text{-PhCCPh})(\eta^6\text{-PhMe})(\mu\text{-CO})(CO)_9$] (7). Anal. Calcd for $C_{37}H_{24}N_2O_{10}Ru_5$ (fw = 1161.94): C, 38.25; H, 2.08; N, 2.41. Found: C, 38.22; H, 2.03; N, 2.43. Positive FAB MS: *m/z* 1163 [M$^+$]. IR (CH_2Cl_2): ν(CO) 2060 (s), 2015 (vs), 2000 (s), 1993 (s, sh), 1982 (m, sh), 1966 (w), 1956 (w), 1943 (w), 1917 (w, br), 1825 (w, br) cm^{-1}. ^{1}H NMR ($CDCl_3$): δ 7.19 (t, J = 7.6 Hz, 1 H, ampy), 7.01 (t, J = 7.6 Hz, 1 H, Ph), 6.9−6.6 (m, 6 H, Ph), 6.54 (d, J = 7.6 Hz, 1 H, ampy), 6.34 (d, br, J = 7.6 Hz, 1 H, Ph), 6.3−6.2 (m, 2 H, Ph), 6.1−5.9 (m, 2 H, ampy and toluene), 5.67 (d, J = 5.6 Hz, 1 H, toluene), 5.57 (t, J = 5.6 Hz, 1 H, toluene), 5.13 (t, J = 5.6 Hz, 1 H, toluene), 4.71 (d, J = 5.6 Hz, 1 H, toluene), 2.61 (s, 3 H, ampy), 2.10 (s, 3 H, toluene).

X-ray Structures of Compounds 2·0.5CH_2Cl_2, 3, 5·0.4CH_2Cl_2, and 7. A selection of crystal, measurement, and refinement data is given in Table 2. Diffraction data were measured at room temperature on a Bruker AXS SMART 1000 diffractometer, using graphite-monochromated Mo Kα radiation. Raw frame data were integrated with SAINT.[24] Absorption corrections were applied with SADABS.[25] Structures were solved by direct methods and refined by full-matrix least squares against F^2 with SHELXTL.[26] All non-hydrogen atoms were refined anisotropically, except the C(8) and C(18) atoms of **5**·0.4CH_2Cl_2, which were kept isotropic due to their tendency to give nonpositive definite ellipsoids. Hydrogen atoms were set in calculated positions and refined as riding atoms. The crystal of **3** was a racemic twin and was refined using the TWIN order. The molecular plots were made with the PLATON program package.[27] The WINGX program system[28] was used throughout the structure determinations. CCDC deposi-

(24) SAINT+: SAX Area Detector Integration Program, Version 6.02; Bruker AXS, Inc., Madison, WI, 1999.

(25) Sheldrick, G. M. SADABS, Empirical Absorption Correction Program; University of Göttingen, Göttingen, Germany, 1997.

(26) Sheldrick, G. M. SHELXTL, An Integrated System for Solving, Refining, and Displaying Crystal Structures from Diffraction Data, Version 5.1; Bruker AXS, Inc., Madison, WI, 1998.

(27) Spek, A. L. PLATON: A Multipurpose Crystallographic Tool; University of Utrecht, Utrecht, The Netherlands, 2003.

(28) Farrugia, L. J. *J. Appl. Crystallogr.* **1999**, *32*, 837.

tion numbers: 253700 (**2**·0.5CH_2Cl_2), 253701 (**3**), 253703 (**5**·0.4CH_2Cl_2), and 253705 (**7**).

X-ray Structures of 4·0.75CH_2Cl_2 and 6. A selection of crystal, measurement, and refinement data is given in Table 2. Diffraction data were collected on a Nonius Kappa-CCD diffractometer, using graphite-monochromated Cu Kα radiation. Raw frame data were integrated with DENZO and SCALEPACK.[29] Empirical absorption corrections were applied using SORTAV.[30] The structures were solved by Patterson interpretation using the program DIRDIF-96.[31] Isotropic and full-matrix anisotropic least-squares refinements against F^2 were carried out using SHELXL-97.[32] Two crystallographically independent cluster molecules were found in the asymmetric unit of **4**·0.75CH_2Cl_2. All non-H atoms were refined anisotropically, except C(90) and C(402) of **4**·0.75CH_2Cl_2, which were treated isotropically due to their tendency to give nonpositive definite ellipsoids. The H atoms of the disordered solvent molecules of **4**·0.75CH_2Cl_2 were not included in the final model. The remaining H atom positions were geometrically calculated and refined riding on their parent atoms. The crystal of **6** was a racemic twin and was refined using the TWIN order. The molecular plots were made with the PLATON program package.[27] The WINGX program system[28] was used throughout the structure determinations. CCDC deposition numbers: 253702 (**4**·0.75CH_2Cl_2) and 253704 (**6**).

Acknowledgment. This work was supported by the Spanish MCyT research projects BQU2002-2623 (to J.A.C.) and BQU2002-03414 (to D.M.). P.G.-A. is also grateful to MCyT for an FPI predoctoral fellowship.

Supporting Information Available: Crystallographic data in CIF format for compounds **2**−**7**. This material is available free of charge via the Internet at http://pubs.acs.org.

OM049186R

(29) Otwinowski, Z.; Minor, W. *Methods Enzymol.* **1997**, *276*, 307.
(30) Blessing, R. H. *Acta Crystallogr., Sect. A* **1995**, *51*, 33.
(31) Beurskens, P. T.; Beurskens, G.; Bosman, W. P.; de Gelder, R.; García-Granda, S.; Gould, R. O.; Israël, R.; Smits, J. M. M. The DIRDIF-96 Program System; Crystallography Laboratory, University of Nijmegen, Nijmegen, The Netherlands, 1996.
(32) Sheldrick, G. M. SHELXL97, Version 97-2; University of Göttingen, Göttingen, Germany, 1997.